

Supporting Information

Enhanced anodic electrochemiluminescence of CdTe quantum dots based on electrocatalytic oxidation of co-reactant by dendrimer encapsulated Pt nanoparticles and its application for sandwiched immunoassays

Lu-Lu Ren^a, Hao Dong^a, Ting-Ting Han^a, Yun Chen^b and Shou-Nian

Ding^{a*}

^aSchool of Chemistry and Chemical Engineering, Southeast University, Nanjing 211189, China

^bDepartment of Immunology, Nanjing Medical University, Nanjing, Jiangsu Province 210029, China

*Corresponding authors. (S.-N. Ding) Fax: (+86)25-52090621. E-mail: snding@seu.edu.cn.

CONTENS

Experimental Section	Page
Reagents and chemicals	S-3
Synthesis of CdTe QDs in aqueous	S-4
Results and Discussion	
Fig. S1. TEM image of Pt DENs	S-5
Fig. S2. UV-vis spectra and FL intensity of CdTe QDs	S-6
Fig. S3. TEM image of CdTe QDs	S-7
Fig. S4. CV curves of Pt DENs in TPrA solution	S-8
Fig. S5. Optimization experimental parameters	S-9
Fig. S6. Stability of the ECL emission of CdTe QDs-Nafion/Pt DENs/GCE	S-10
Fig. S7. TEM image of Fe ₃ O ₄ @SiO ₂ nanoparticles	S-11
Fig. S8. TEM image of Fe ₃ O ₄ @SiO ₂ /Pt DENs nanocomposites	S-12
Fig. S9. FT-IR spectra of the Fe ₃ O ₄ @SiO ₂ before and after amination	S-13
Fig. S10. Magnetization curves of Fe ₃ O ₄ , Fe ₃ O ₄ @SiO ₂ and Fe ₃ O ₄ @SiO ₂ -Pt DENs	S-14
Fig. S11. UV-vis spectra of the construction of captured probe	S-15
Fig. S12. Optimization of pH, amount of QDs and incubation time	S-16
Fig. S13. Stability, reproducibility and specificity of immunosensor	S-17
Table S1. Comparison of different immunosensors for CEA detection	S-18
Table S2. Detection of CEA using ELISA method and proposed immunosensor	S-19
Table S3. Assay results of CEA in real samples	S-20
References	S-21

Reagents and chemicals. Cadmium Chloride ($\text{CdCl}_2 \cdot 2.5\text{H}_2\text{O}$, >99.0%) was obtained from Shanghai Jinshan Tingxin Chemical Reagent Co. Ltd. (Shanghai, China). Sodium borohydride (NaBH_4 , $\geq 96.0\%$), tellurium powder (Te, 99.9%), trisodium citrate dehydrate ($\text{Na}_3\text{Cit} \cdot 2\text{H}_2\text{O}$), $\text{FeCl}_3 \cdot 6\text{H}_2\text{O}$, ethylene glycol (EG) and sodium acetate anhydrous (NaAc) were provided from Sinopharm Chemical Reagents Co. Ltd, (Shanghai, China). 3-Mercaptopropionic acid (MPA, 98.0%), tripropylamine, (3-aminopropyl) triethoxysilane (APTES, 97%), ethyl silicate (TEOS) and glutaraldehyde (GA, 25%) were obtained from Aladdin Industrial Corporation. N-(3-dimethylaminopropyl)-N'-ethylcarbodiimide hydrochloride (EDC) and N-hydroxysuccinimide (NHS) were purchased from Sigma-Aldrich. Bovine serum albumin (BSA) was obtained from Sangon Biotech Co., Ltd.

Synthesis of CdTe QDs in aqueous. CdTe QDs capped with 3-Mercaptopropionic acid (MPA) were synthesized according to the literatures^{1, 2}. Briefly, 67.0 μL of MPA and 91.3 mg of $\text{CdCl}_2 \cdot 2.5 \text{H}_2\text{O}$ were dissolved in 40 mL of H_2O . The pH of solution was adjusted to 11.0 using 1.0 M NaOH. Under stirring with N_2 , the 1.0 mL of freshly prepared 0.04 M NaHTe solution (produced by the reaction of oxygen-free NaBH_4 solution with Te powder under N_2 atmosphere) was added to this solution at room temperature. Then the solution was refluxed at 100 $^\circ\text{C}$. The obtained CdTe products were precipitated for three times by ethanol with centrifugation at 10,000 rpm for 10 min. The purified CdTe precipitates were dispersed in deionized water and stored at 4 $^\circ\text{C}$ for later use.

Fig. S1 TEM image of as-synthesized Pt DENs (inset: particle size distribution histogram of Pt DENs).

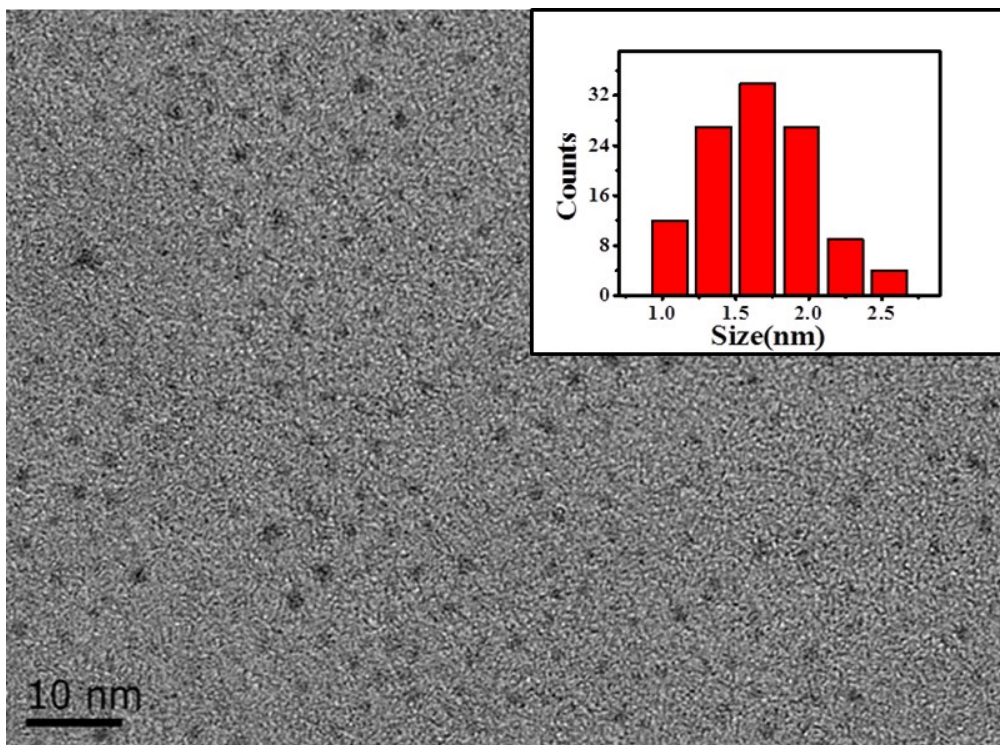


Fig. S2 Normalized UV-vis absorption spectra and normalized FL intensity of CdTe QDs.

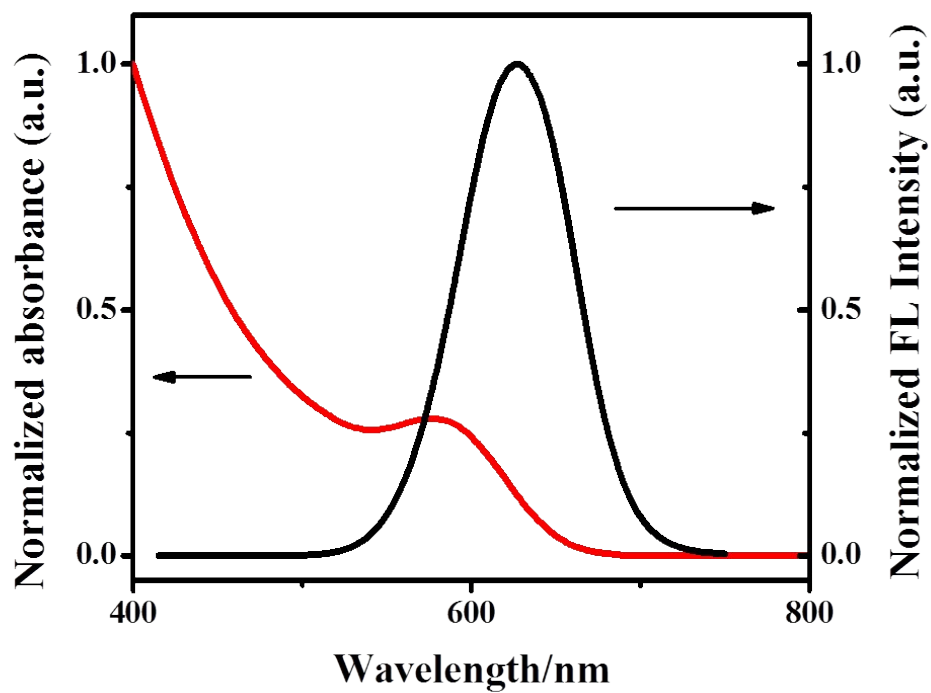


Fig. S3 TEM image of as-synthesized CdTe QDs.

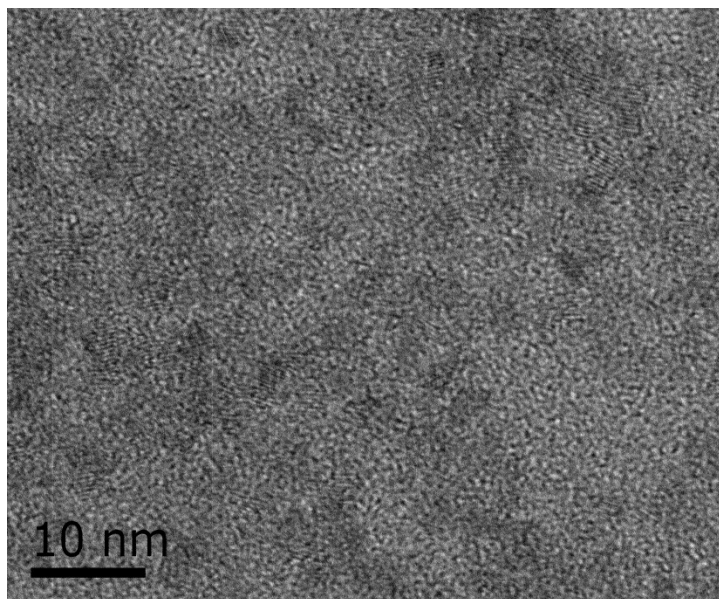


Fig. S4 CV curves of (a) bare GCE, (b) Pt DENs/GCE in 0.1 M PBS (pH 7.5); (c) bare GCE, (d) Pt DENs/GCE in 0.1 M PBS (pH 7.5) containing 10 mM TPrA. The volume of Pt DENs used to modify GCE is 5 μ L.

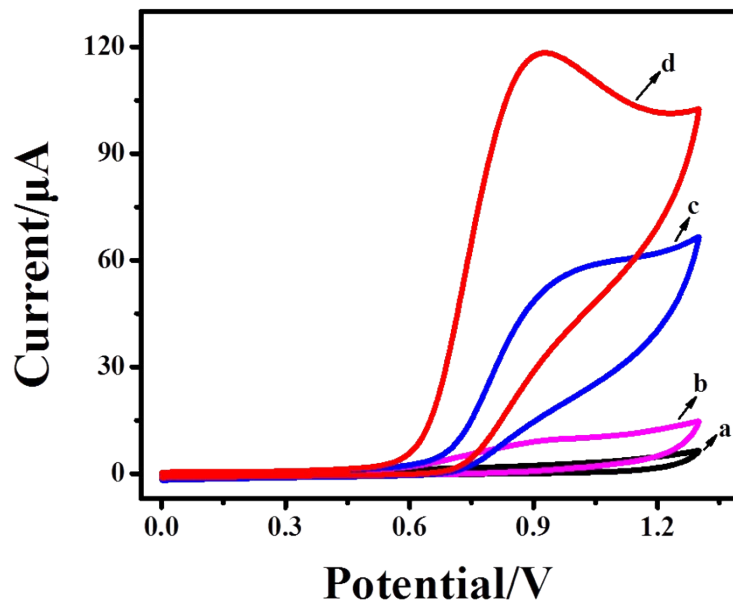


Fig. S5 (A) The ECL intensity of CdTe QDs-Nafion/Pt DENs/GCE fabricated by dropping the mixture containing 1mg/mL QDs, 5 μ L of as-diluted Pt DENs and different concentration of Nafion in 0.1 M PBS (pH 7.5) containing 10 mM TPrA. (B) The ECL intensity of CdTe QDs-Nafion/Pt DENs/GCE fabricated by dropping the mixture containing 1 mg/mL QDs, 0.2 mg/mL Nafion and different volume of Pt DENs in 0.1 M PBS (pH 7.5) containing 10 mM TPrA. (C) The ECL intensity of CdTe QDs-Nafion/Pt DENs/GCE fabricated in different pH value of 0.1 M PBS containing 10 mM TPrA.

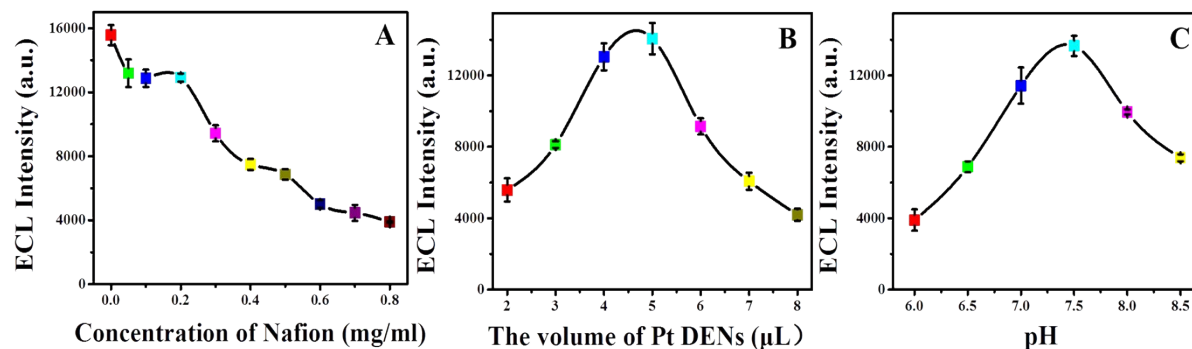


Fig. S6 Stability of the ECL emission of CdTe QDs-Nafion/Pt DENs/GCE under continuous cyclic potential (PMT 450V).

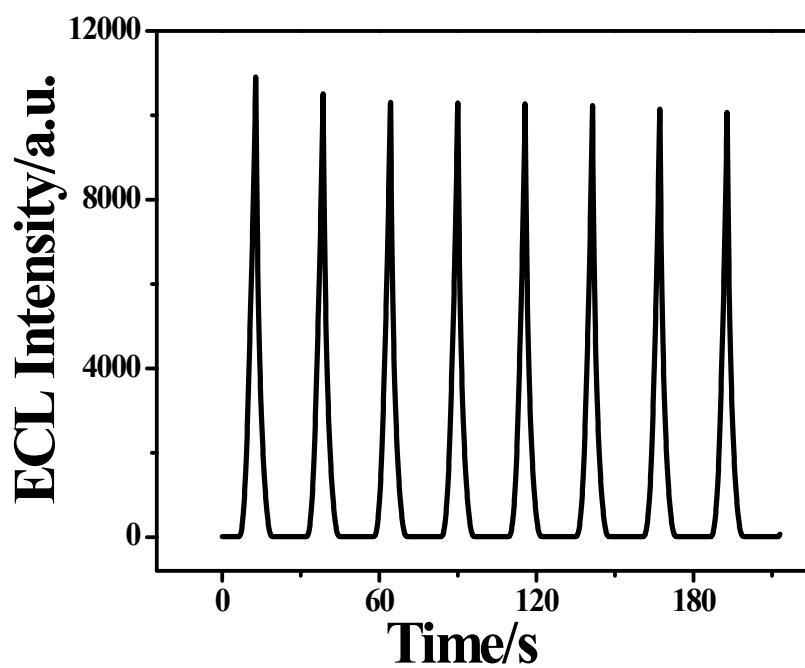


Fig. S7 TEM image of $\text{Fe}_3\text{O}_4@\text{SiO}_2$ nanoparticles.

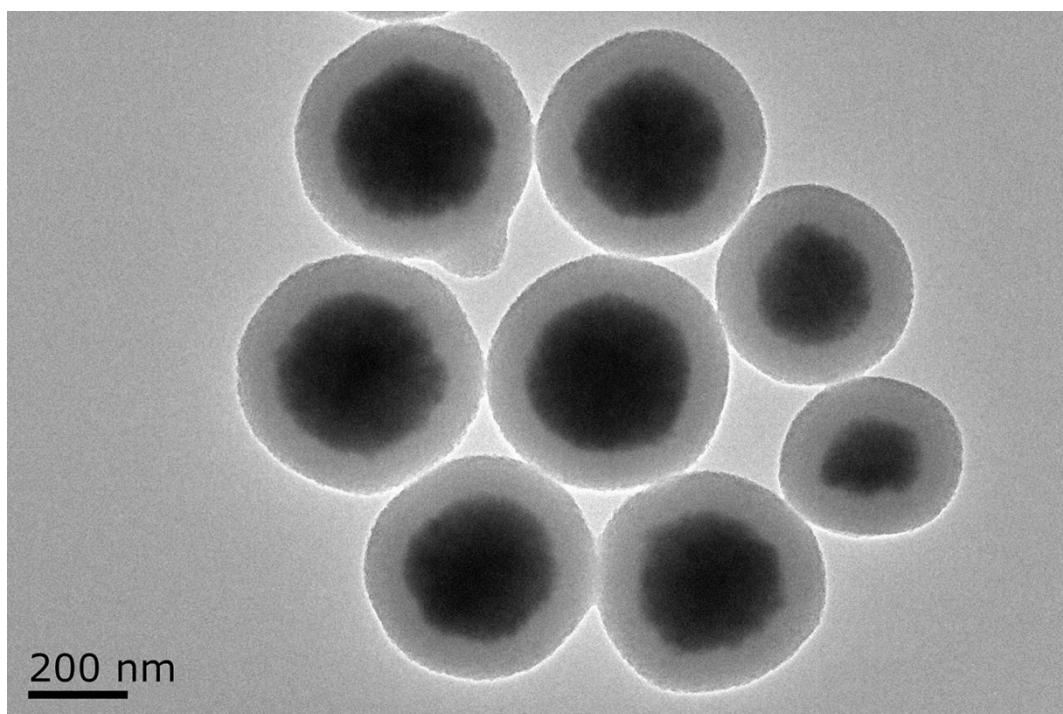


Fig. S8 TEM image of $\text{Fe}_3\text{O}_4@\text{SiO}_2/\text{Pt}$ DENs nanocomposites without cross-linking treatment.

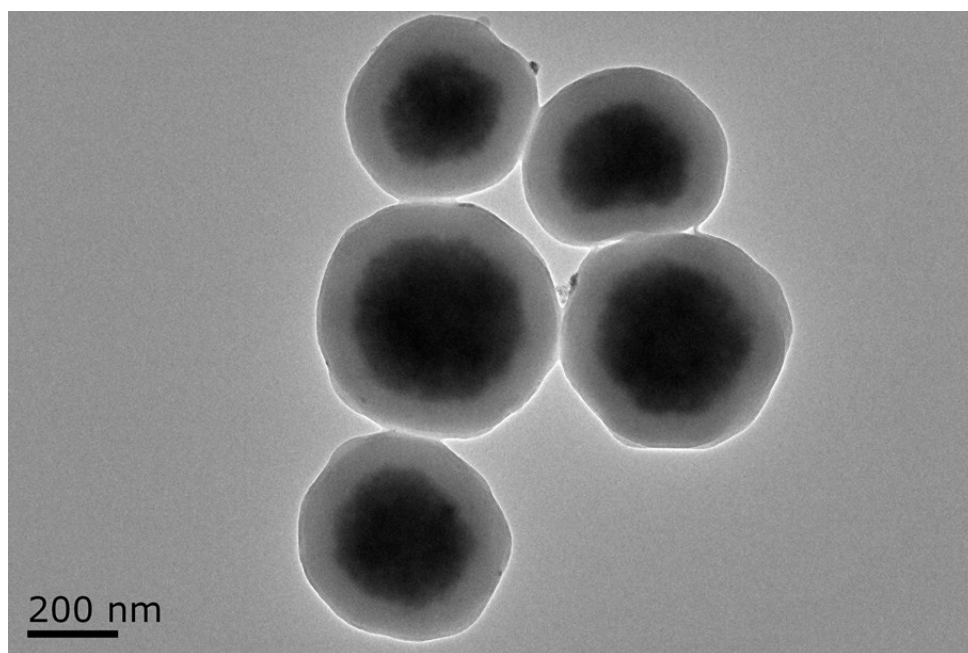


Fig. S9 FT-IR spectra of the $\text{Fe}_3\text{O}_4@\text{SiO}_2$ nanoparticles before and after surface modification with APTES.

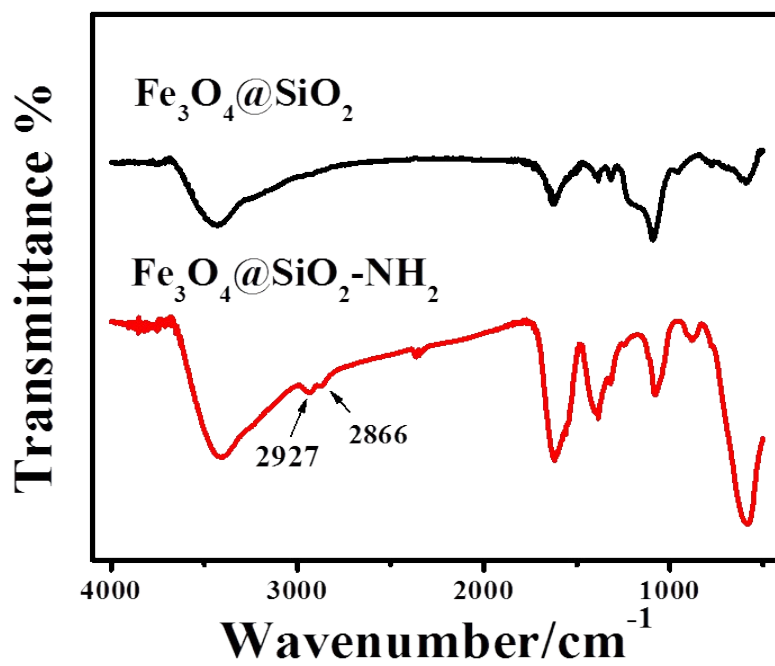


Fig. S10 Magnetization curves of Fe_3O_4 NPs (a), $\text{Fe}_3\text{O}_4@$ SiO_2 NPs (b) and $\text{Fe}_3\text{O}_4@$ SiO_2 -Pt DENs nanocomposites (c) measured at 298 K. Insets: the photographs of $\text{Fe}_3\text{O}_4@$ SiO_2 -Pt DENs nanocomposites before and after magnetic separation by an external magnet.

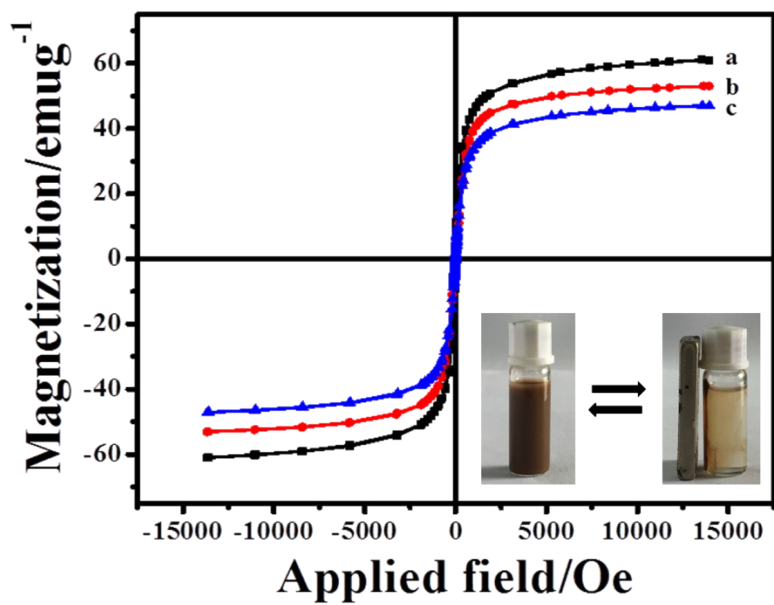


Fig. S11 UV-vis spectra of Fe₃O₄@SiO₂ (a), Pt DENs (b), Fe₃O₄@SiO₂-Pt DENs (c), Ab₁ (d) and Fe₃O₄@SiO₂-Pt DENs/Ab₁ conjugation (e).

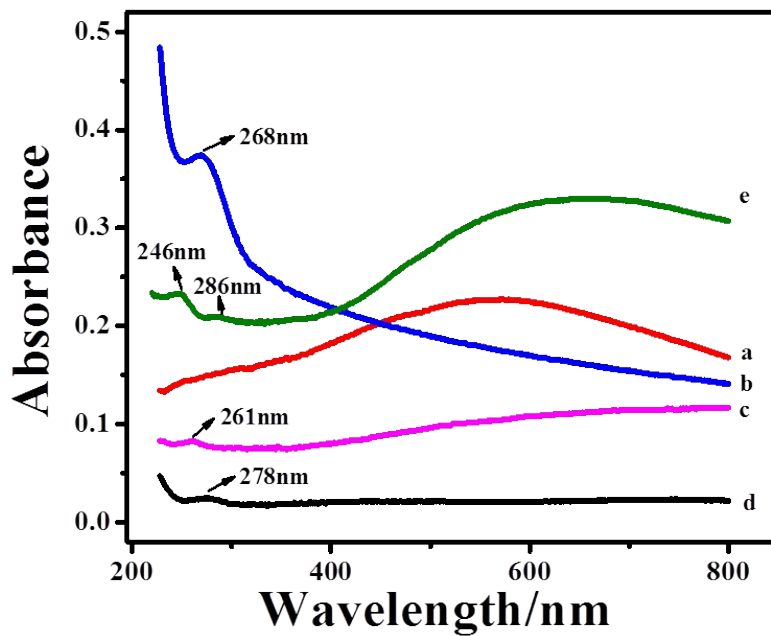


Fig. S12 Effects of pH (A), the amount of QDs added during labeling (B) and incubation time (C) on the ECL intensity of immunosensor. (a) Incubation with Ag, (b) Incubation with QDs-Ab₂.

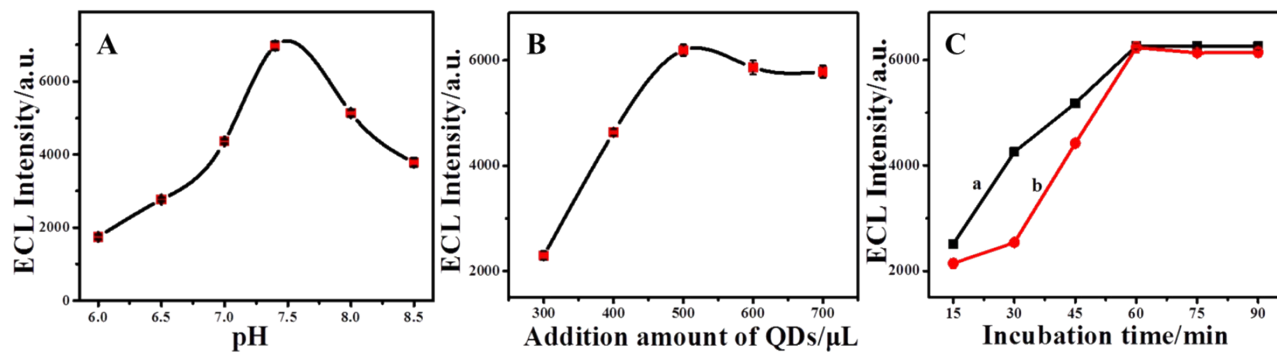


Fig. S13 (A) ECL signals under continuous scan at different concentrations of CEA. (B) Storage stability of the immunosensor. (C) The study on the reproduction of the immunosensor. (D) Specificity investigations of the immunosensor for CEA detection: (a) blank, (b) Human IgG (500 ng/mL), (c) AFP (500 ng/mL), (d) BSA (500 ng/mL), (e) CEA (50 ng/mL), (f) CEA (50 ng/mL) + Human IgG (500 ng/mL), (g) CEA (50 ng/mL) + AFP (500 ng/mL), (h) CEA (50 ng/mL) + BSA (500 ng/mL).

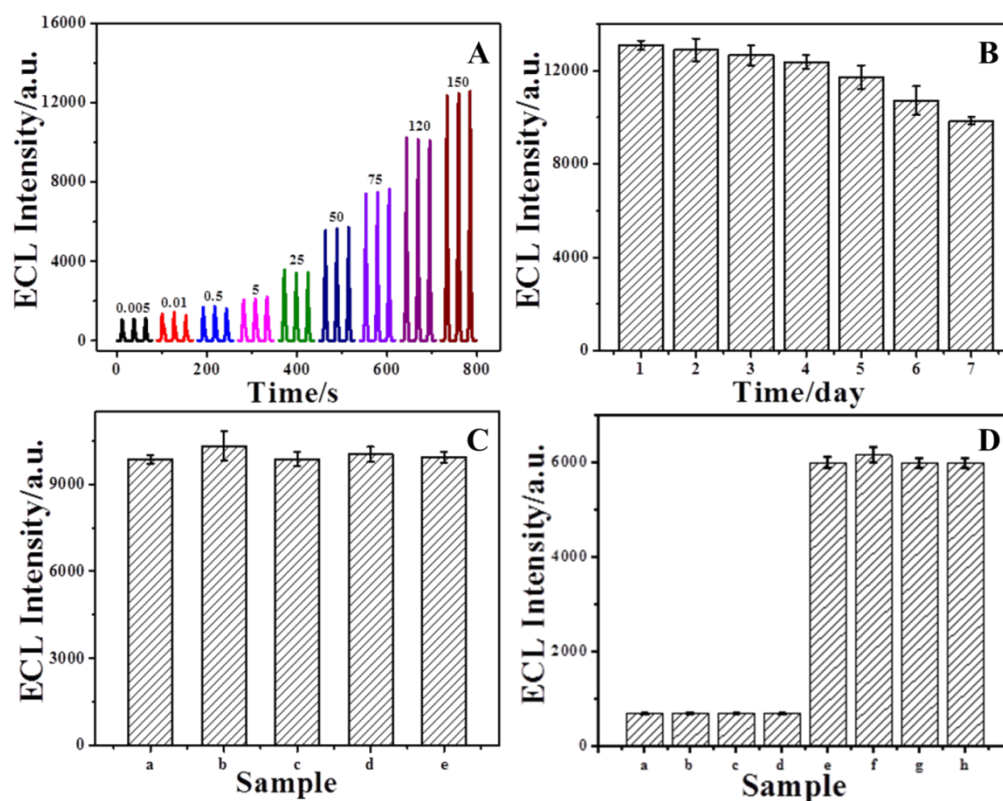


Table S1 The proposed ECL immunosensors for detecting CEA compared to other published ECL immunosensor.

Materials, methods	Linear ranges	Detection limit	Ref.
Au@BSA core/shell nanoparticles, ECL	0.001-200 ng/mL	0.3 pg/mL	3
g-C ₃ N ₄ nanosheets, pH indicator	0.5-100 ng/mL	0.34 pg/mL	4
Silver nanoclusters, Fluorescence	0.01-1 ng/mL	3 pg/mL	5
Graphene Oxide-BaYF ₅ :Yb, ECL	0.001-80 ng/mL	0.87 pg/mL	6
Gold composite, Electrochemical	1-150 ng/mL	0.2 ng/mL	7
Polythionine-gold, Electrochemical	0.005-40 ng/mL	2.2 pg/mL	8
Thiol derivative nanogold, Ultraviolet (UV) spectroscopy	5-80 ng/ml	2 pg/mL	9
CdTe QDs and AuNPs, ECL	0.01-40 ng/mL	1.67 pg/mL	10
This method	0.005-150 ng/ml	0.2 pg/mL	-

Table S2 The detection for CEA in real samples using the proposed immunosensor and the commercial ELISA method.

Sample No.	Commercial ELISA method (ng/mL)	Our method (ng/mL)	Relative derivation (%)
1	1.45	1.51	4.14
2	3.12	3.23	3.53
3	100.21	103.14	2.92

Table S3 The results of CEA detection in serum samples.

	Initial human serum (ng/mL)	The addition content (ng/mL)	The detection content (ng/mL)	RSD/ %, n=3	Recovery/ %
1	0.30	0.24	0.25	3.84	104.17
		0.30	0.29	2.98	96.7
		0.36	0.38	4.12	105.56
2	0.65	0.52	0.50	5.96	96.15
		0.65	0.67	2.13	103.08
		0.78	0.82	3.09	105.13
3	20.63	16.50	17.13	4.18	103.82
		20.63	20.67	5.12	100.19
		24.76	25.39	4.45	102.54

References

- 1 X. Zhang and S.-N. Ding, *ACS Sens.*, 2016, **1**, 358-365.
- 2 L. Zou, Z. Gu, N. Zhang, Y. Zhang, Z. Fang, W. Zhu and X. Zhong, *J. Mater. Chem.*, 2008, **18**, 2807.
- 3 A. Zhang, C. Huang, H. Shi, W. Guo, X. Zhang, H. Xiang, T. Jia, F. Miao and N. Jia, *Sens. Actuators, B*, 2017, **238**, 24-31.
- 4 F. Shao, L. Jiao, L. Miao, Q. Wei and H. Li, *Biosens. Bioelectron.*, 2017, **90**, 1-5.
- 5 X. Yang, Y. Zhuo, S. Zhu, Y. Luo, Y. Feng and Y. Xu, *Biosens. Bioelectron.*, 2015, **64**, 345-351.
- 6 L. Zhao, J. Li, Y. Liu, Y. Wei, J. Zhang, J. Zhang, Q. Xia, Q. Zhang, W. Zhao and X. Chen, *Sens. Actuators, B*, 2016, **232**, 484-491.
- 7 J. Shan and Z. Ma, *Microchim. Acta*, 2016, **183**, 2889-2897.
- 8 X. Cai, S. Weng, R. Guo, L. Lin, W. Chen, Z. Zheng, Z. Huang and X. Lin, *Biosens. Bioelectron.*, 2016, **81**, 173-180.
- 9 H. Zeng, D. A. Y. Agyapong, C. Li, R. Zhao, H. Yang, C. Wu, Y. Jiang and Y. Liu, *Sens. Actuators, B*, 2015, **221**, 22-27.
- 10 M. Yang, Y. Chen, Y. Xiang, R. Yuan and Y. Chai, *Biosens. Bioelectron.*, 2013, **50**, 393-398.